Two-dimensional modelling of laminated piezoelectric composites: analysis and numerical results

Amâncio Fernandes, Joël Pouget

Two-dimensional modelling of laminated piezoelectric composites : Analysis and numerics

Amâncio FERNANDES and Joël POUGET

Laboratoire de Modélisation en Mécanique (UMR 7607)
Université Pierre et Marie Curie, Case 162, 4 Place Jussieu
75252 Paris Cedex 05, France

Abstract - We propose a new approach to laminated piezoelectric plates based on a refinement of the electric potential as function of the thickness coordinate of the laminate and accounting for shear effects. Moreover, the variation of the electric potential as function of the thickness coordinate is modelled for each layer of the laminate. The equation for the laminated piezoelectric plate are then obtained by using a variational formulation involving mechanical surface loads or prescribed electric potential on the top and bottom faces of the plate. In addition to the equations for the generalized stress resultants (due to the shear effects), the equation of the electric charge conservation is also deduced for the 2D model.
A particular attention is devoted to the single piezoelectric plate and bimorph structure and the through-thickness distribution of the displacements, electric potential as well as stresses are given for different kinds of electromechanical loads. The results thus obtained are compared to those provided by a finite element method performed for the full 3D model. A good agreement is observed for plates made of layers of PZT-4 piezoelectric material. The comparison ascertains the effectiveness of the present 2D approach to piezoelectric laminates.
Keywords : piezoelectric plates, adaptive materials, piezoelectric bimorph.

1. Introduction

Application of induced strain actuators are spreading widely in various fields of engineering such as precise positioning, intelligent control of shapes and active damping of vibrations [1-4]. Among the different types of actuators, the *piezoelectric actuators* are the most popular, probably because of their simple and versatile design. The most simple piezoelectric actuator is usually made of single-component system (for instance, a slab of piezoelectric material). Typically, such a actuator produces displacements in the order of 10 to 100 μm when applying an electric field of 2 kV/mm. To overcome this limitation, an actuator using flexural-extensional deformation of the structure requires several components and it will be a *composite material* rather than a monolithic structure. One of the advantages of the *multilayer technique* with piezoelectric materials is to induce strain of the order of 1200 p.p.m. by applying voltage less than 200 volts. In order to obtain large amplitude motions in piezoelectric devices, a *bilayer* or *sandwich structure* is commonly used in which a piezoelectric layer, with its direction of polarization perpendicular to the layer faces, is glued back to back with a strip of nonresponsive but elastic layer. The contraction of the piezoelectric layer in response to an applied field will be hindered by the elastic layer and the bilayer composite will bend. This is the reason for modelling and understanding composite structures made of a stacking of piezoelectric plates.

Several versions of linear piezoelectric plate have been proposed by H.F. Tiersten [5], R.D. Mindlin [6] and C.K. Lee [7]. A first approach is based usually on Love's first-approximation including the Gauss equation for the electric charge and extended to laminated plate using first-order shear deformation theory [8]. An interesting refined theory of layerwise approach to the electric potential has been introduced by J.N. Reddy [9]. Nevertheless, most models are based on a classical laminated plate theory which neglects the transverse shear effects. More refined and higher-order theories for piezoelectric plates become a necessity to well understand strain sensing and actuating in piezoelectric laminated plates.
In the present work, we intend to study a refined approach to piezoelectric laminated plate involving *shear effects* and *layerwise description* of the electric potential. The model examined, here, includes the charge equation, so that we do not consider any hypothesis on the electric displacement. The shear distribution across the plate thickness is approximated by a trigonometric function [10]. Our particular choice for the approximation of the displacement field and electric potential must satisfy the boundary conditions. Especially, the plate can be subject either to an applied electric potential on the top and bottom faces of the plate or to a density of force on the top face. However, the boundary conditions can be extended to applied electric charge density as well. A variational formulation is considered to reduce the equations of the full 3D model to those of 2D for the piezoelectric plate. The variational formulation is then generalized to plates made of piezoelectric layers and accounts for the continuity conditions at the layer interfaces.

The next section, Section 2, is devoted to the variational formulation of piezoelectric media. The approximation model is presented in Section 3. In Section 4, the equations for the piezoelectric plate are deduced from the variational formulation and some generalized stress resultants and electric charges are defined, as well. The boundary conditions are discussed in Section 5. A special attention is addressed to a single piezoelectric plate in Section 6. The full equations for the single piezoelectric plate are investigated in Section 7 and the solution for piezoelectric plates in cylindrical bending is presented and the comparison to finite element simulations is also considered. The bilayer structure is given in Section 8, the piezoelectric bimorph structure is studied for different kinds of electromechanical loads. The comparison to numerics by means of finite element method leads to a good accuracy of the present model. At length, by way of conclusion, some extensions of the model and further works are evoked in Section 9.

2. Reminder : variational formulation of piezoelectricity

In this section, we briefly recall all the requisites about piezoelectricity and the associated variational formulation based on Hamilton's principle. The advantage of this method is that it accounts for both the mechanical and electrical aspects simultaneously. Moreover, the formulation considers the natural boundary conditions connected with the mechanical and electrical quantities. The variational principle is stated as [6]

$$\delta \int_{t_1}^{t_2} (L + W) dt = \int_{t_1}^{t_2} (\delta K - \delta U + \delta W) dt = 0 \quad , \tag{1}$$

where L is the Lagrangian, K is the kinetic energy, U is the potential energy and W is the

external work. For a piezoelectric medium the associated potential energy density can be identified with the electric enthalpy density function which can be expressed in terms of the strain and electric field as follows

$$\mathcal{U} = H(\varepsilon_{ij}, E_i) = \frac{1}{2}\sigma_{ij}\varepsilon_{ij} - \frac{1}{2}D_i E_i \quad , \tag{2}$$

where σ_{ij} are the components of the stress tensor, ε_{ij} are the components of the strain tensor, D_i is the electric displacement and E_i is the electric field vector. The stress tensor and the electric displacement vector are derived from the enthalpy

$$\sigma_{ij} = \frac{\partial H}{\partial \varepsilon_{ij}} \quad , \qquad D_i = -\frac{\partial H}{\partial E_i} \quad . \tag{3}$$

The formulation must be completed with the use of the piezoelectric constitutive equations. Here, the study is restricted to the classical linear piezoelectricity within the *electrostatic* framework for which we have $\mathbf{rot}\ \mathbf{E} = \mathbf{0}$ and the electric field is derivable from an electric potential ϕ by

$$E_i = -\phi_{,i} \quad . \tag{4}$$

On using the above definition and assuming there are no body forces the variational formulation takes on the following form

$$-\int_{t_1}^{t_2}\int_{\Omega}(\rho\ddot{u}_i\delta u_i + \sigma_{ij}\delta\varepsilon_{ij} + D_j(\delta\phi)_{,j})dvdt + \int_{t_1}^{t_2}\int_{\partial\Omega}(T_i\delta u_i + q\delta\phi)dSdt = 0 \quad . \tag{5}$$

The second part of Eq.(5) represents the virtual external work involving the surface traction T_i and applied surface electric charge q on the domain boundary $\partial\Omega$. The variational formulation will be applied to derive a set of approximate governing equations for laminated piezoelectric plates by accounting for the approximation of the displacement field and electric potential as function of the thickness coordinate of the plate. In Hamiltonian's principle, it is assumed that the virtual displacements and electric potential are zero at t_1 and t_2. The coupled linear constitutive equations for piezoelectric materials are given by [6]

$$\left\{ \begin{array}{rcl} \sigma_{ij} & = & C^E_{ijkl}\varepsilon_{kl} - e_{kij}E_k \quad , \\ D_i & = & e_{ijk}\varepsilon_{jk} + \chi_{ij}E_j \quad , \end{array} \right. \tag{6}$$

where the strain $\varepsilon_{ij} = u_{(i,j)} = \frac{1}{2}(u_{i,j} + u_{j,i})$ and $\mathbf{u}$ is the displacement vector. In Eq.(6), $\mathbf{C^E}$ is the fourth-order tensor of elasticity coefficients at zero electric field, $\mathbf{e}$ is the third-order tensor of piezoelectricity coefficients and $\boldsymbol{\chi}$ is the second-order tensor of dielectric constants at vanishing strain. In the following, we will focus our attention to materials which possess three mutually perpendicular planes of symmetry, it is referred to as orthotropic. Therefore only the following material coefficients are non zero (we use the Voigt notation with indices)

$$\begin{array}{l} C^E_{\alpha\beta} = \{C^E_{11}, C^E_{12}, C^E_{13}, C^E_{22}, C^E_{23}, C^E_{33}, C^E_{44}, C^E_{55}, C^E_{66}\} \quad , \\ e_{i\alpha} = \{e_{15}, e_{24}, e_{31}, e_{32}, e_{33}\} \quad , \\ \chi_{ij} = \{\chi_{11}, \chi_{22}, \chi_{33}\} \quad . \end{array}$$

If the material system has an axis of symmetry (hexagonal system) the number of independant material coefficients is reduced according to $C^E_{11} = C^E_{22}$, $C^E_{13} = C^E_{23}$, $C^E_{44} = C^E_{55}$

and $C_{66}^E = \frac{1}{2}(C_{11}^E - C_{12}^E)$, $e_{31} = e_{32}$, $e_{15} = e_{24}$, and $\chi_{11} = \chi_{22}$.

3. Approximation of the displacement field and electric potential

Most plate models consider an expansion of the displacements in power series of the thickness coordinate. The level of truncation of the expansion leads to the order of the plate theory. In the present model, the displacement field and electric potential are assumed to be of the form

$$\left\{\begin{array}{lcl} u_\alpha(x,y,z,t) &=& U_\alpha(x,y,t) - z w_{,\alpha}(x,y,t) + f(z)\gamma_\alpha(x,y,t), \quad \alpha \in \{1,2\} \quad , \\ u_3(x,y,z,t) &=& w(x,y,t) \quad , \\ \phi(x,y,z,t) &=& \phi_0(x,y,t) + z\phi_1(x,y,t) + P(z)\phi_2(x,y,t) + g(z)\phi_3(x,y,t) \quad . \end{array}\right. \tag{7}$$

Some comments on the above expansions are in order, (i) $f(z) = 0$, we recover the classical Kirchhoff-Love thin plate theory [11], (ii) at the first order in the expansion of $f(z)$, $f(z) = z$ we obtain the Mindlin-Reissner model [12] and (iii) the expansion of $f(z)$ to the third order leads to a refined model of the same order as that of M. Levinson [13] and J.N. Reddy [14]. In the present approach, we have considered

$$f(z) = \frac{h}{\pi}\sin\left(\frac{\pi z}{h}\right), \qquad g(z) = \frac{h}{\pi}\cos\left(\frac{\pi z}{h}\right), \qquad P(z) = z^2 - \left(\frac{h}{2}\right)^2 \quad , \tag{8}$$

where h is the plate thickness which is supposed to be uniform. The case of the purely elastic plates has been extensively examined by M. Touratier [10] and extended to elastic shells [15].
In the approximation of the electric potential, the first two terms, the linear part, can be connected with the applied electric potential. The third term represents the induced electric potential by material deformation through piezoelectric coupling. Such a quadratic term has been suggested by J.S. Yang [16] and N.N. Rogacheva [17]. The last term corresponds to the shearing effects approximated by the function $f(z)$ in the displacement. Most theories of piezoelectric plate are limited to a classical Kirchhoff-Love model for the elastic part and to the linear approximation for the electric potential. Some approaches are based on discrete layer approximation for the electric potential using Lagrange interpolation functions [18]. They are equivalent to finite element methods. In the present approach, we point out the usefulness of the refinement introduced in the approximation of the elastic displacements and electric potential, especially if the plate is not really thin.

4. Boundary conditions

Two kinds of electromechanical boundary conditions are considered on the top and bottom faces of the plate :
(a) an electric potential is applied on the plate faces, such as

$$\phi(x,y,z = \pm h/2,t) = V^{\pm}(x,y,t) \quad . \tag{9}$$

Since $P(\pm h/2) = 0$ and $g(\pm h/2) = 0$ (see Eq.(8)), the boundary conditions (9) yield

$$\phi_0 = \frac{1}{2}\left(V^+ + V^-\right) \quad \text{and} \quad \phi_1 = \frac{1}{h}\left(V^+ - V^-\right) \quad . \tag{10}$$

Accordingly, the functions ϕ_0 and ϕ_1 are not arbitrary and they depend on the applied electric potential. For the sake of simplicity, we take $V^+ = V$ and $V^- = -V$ so that we

have $\phi_0 = 0$ and $\phi_1 = 2V/h$. Moreover, the applied electric potential is supposed to be uniform.
(b) The second kind of boundary condition is a charge density of force p per unit area and perpendicular to the plate faces.

Remarks. The Maxwell equations for the electromagnetic fields lead to the associated boundary conditions [19], especially for the electric field ($[\![\mathbf{E}]\!] \times \mathbf{n} = \mathbf{0}$), which imposes the continuity of the tangential component of the electric field through the interface. In order to apply the electric potential, the top and bottom faces of the plate are coated with thin metallic electrodes of negligeable thickness and playing no role mechanically. Nevertheless, it is assumed that the stresses and displacements are perfectly transmitted through the electrodes. Therefore, the potential is uniform on the electrode. Since in a conductor the electric field is zero, the boundary condition on the electric field can be written as $E_1 = E_2 = 0$ on the top and bottom faces of the plate. At last, it is worthwhile noting that electric charges can be imposed on the top and bottom of the plate, in this situation the boundary conditions on the electric displacement is $[\![\mathbf{D}]\!] \cdot \mathbf{n} = q$, which is, in our case, read as $D_3(\pm h/2) = q$.

5. The plate equations

The variational formulation presented in Section 2 is used to derive a *two-dimensional model* from the fully three-dimensional theory of piezoelectricity. By substituting the approximation made for the displacement field and electric potential as given in Section 3, it is possible to eliminate the dependency of the field on the thickness coordinate z. To obtain the equations and boundary conditions for the two-dimensional model, displacement and electric potential approximations (see Eq.(7)) along with the boundary conditions (10) are substituted into the variational principle (5). The dependency on z is integrated out by introducing generalized stress and electric charge resultants. The variational formulation can be written as

$$\int_{t_1}^{t_2} \left(-\delta U + \delta W_1 + \delta W_2\right) dt = 0 \quad . \tag{11}$$

In the present study only static processes are investigated so that the kinetic energy is dropped out. The first term in Eq.(11) is the variation of the internal force work

$$\begin{aligned} \delta U = \int_\Sigma \{ & N_{\alpha\beta} \left(\delta U_\alpha\right)_{,\beta} - M_{\alpha\beta} \left(\delta w\right)_{,\alpha\beta} + \hat{M}_{\alpha\beta} \left(\delta\gamma_\alpha\right)_{,\beta} + \hat{Q}_\alpha \delta\gamma_\alpha \\ & + D_\alpha^{(2)} \left(\delta\phi_2\right)_{,\alpha} + D_\alpha^{(3)} \left(\delta\phi_3\right)_{,\alpha} + D_3^{(2)} \delta\phi_2 + D_3^{(3)} \delta\phi_3 \} dS \quad . \end{aligned} \tag{12}$$

In the above variation we have introduced some stress and electric charge or induction resultants as follows

$$\left(N_{\alpha\beta}, M_{\alpha\beta}, \hat{M}_{\alpha\beta}\right) = \int_{-h/2}^{+h/2} \left(1, z, f(z)\right) \sigma_{\alpha\beta} dz \quad , \tag{13}$$

$$\hat{Q}_\alpha = \int_{-h/2}^{+h/2} f'(z) \sigma_{\alpha 3} dz \quad , \tag{14}$$

for $\alpha, \beta \in \{1,2\}$ and $f'(z) = \frac{df(z)}{dz}$. In addition, we have

$$\left(D_\alpha^{(2)}, D_\alpha^{(3)}\right) = \int_{-h/2}^{+h/2} \left(P(z), g(z)\right) D_\alpha dz \quad , \tag{15}$$

$$\left(D_3^{(2)}, D_3^{(3)}\right) = \int_{-h/2}^{+h/2} \left(P'(z), g'(z)\right) D_3 dz \quad , \tag{16}$$

with $P'(z) = \frac{dP(z)}{dz}$ and $g'(z) = \frac{dg(z)}{dz}$. Finally, the last two terms in Eq.(11) denote the variation of the works of applied forces and electric charges on the plate boundary which is the sum of the works of the forces and electric charges applied on the top and bottom faces of the plate and those of the same quantities applied on the lateral boundary of the plate, namely

$$\delta W_1 = \int_\Sigma \left(f_\alpha \delta U_\alpha - p\delta w + \hat{m}_\alpha \delta\gamma_\alpha\right) dS \quad , \tag{17}$$

$$\delta W_2 = \int_{\mathcal{C}} \left(F_\alpha \delta U_\alpha + T\delta w + C_\alpha \delta\gamma_\alpha - M_f \left(\delta w\right)_{,n}\right) d\ell - \sum_p Z_p \delta w_p \quad . \tag{18}$$

In Eq.(17), f_α and p are densities of force per unit of area, $\hat{m}_\alpha$ is a surface moment density. In Eq.(18), F_α and T are densities of force per unit of length, M_f and C_α are lineic moment densities and Z_p are transverse forces applied at angular points of the edge boundary contour $\mathcal{C}$ of the plate. In Eq.(18) $\left(\delta w\right)_{,n}$ is the derivative of the variation δw with respect to the normal direction to the boundary contour. The electric charges on the top and bottom faces of the plate do not appear explicitly in the virtual works (they are cancelled out by integrating on the plate thickness).

In order to obtain the Euler-Lagrange equations from the variational formulation, we use integration by parts if needed and we collect the factors of the arbitrary variations $\{\delta U_\alpha, \delta w, \delta\gamma_\alpha, \delta\phi_2, \delta\phi_3\}$. By assuming that the variational formulation holds for any arbitrary variations, we obtain the following set of equations (for the static case)

$$\left\{\begin{array}{l} N_{\alpha\beta,\beta} + f_\alpha = 0 \quad , \\ M_{\alpha\beta,\alpha\beta} - p = 0 \quad , \\ \hat{M}_{\alpha\beta,\beta} - \hat{Q}_\alpha + \hat{m}_\alpha = 0 \quad , \end{array}\right. \tag{19}$$

and

$$\left\{\begin{array}{l} D_{\alpha,\alpha}^{(2)} - D_3^{(2)} = 0 \quad , \\ D_{\alpha,\alpha}^{(3)} - D_3^{(3)} = 0 \quad . \end{array}\right. \tag{20}$$

The associated boundary conditions on the plate edge $\mathcal{C}$ are given by

$$\left\{\begin{array}{lcllll} F_\alpha & = & N_{\alpha\beta} n_\beta & \text{or} & U_\alpha & \text{given} \quad , \\ T & = & \left(\tau_\alpha M_{\alpha\beta} n_\beta\right)_{,s} + n_\alpha M_{\alpha\beta,\beta} & \text{or} & w & \text{given} \quad , \\ M_f & = & n_\alpha M_{\alpha\beta} n_\beta & \text{or} & w_{,n} & \text{given} \quad , \\ C_\alpha & = & \hat{M}_{\alpha\beta} n_\beta & \text{or} & \gamma_\alpha & \text{given} \quad , \\ D_\alpha^{(A)} n_\alpha & = & 0 \quad (A \in \{2,3\}) & \text{or} & \phi_A & \text{given} \quad , \end{array}\right. \tag{21}$$

and at the angular points A_p of the edge we write $[\![\tau_\alpha M_{\alpha\beta} n_\beta - Z_p]\!]_{A_p} = 0$. In Eqs.(21) $\boldsymbol{\tau}$ is the tangent vector to the edge contour $\mathcal{C}$.
The first two equations in Eq.(19) are strictly equivalent to those of the Kirchhoff-Love model for the classical plate theory [12]. The third equation governs the shearing effects. Equations (20) are deduced from the electric charge balance law. Moreover, it has been supposed no electric charge on the lateral edge of the plate contour (no electrode), because the dielectric constant of the piezoelectric plate is much larger than the dielectric constant of the outside air. Accordingly the left hand side of Eq.$(21)_5$ is zero.

5. The plate constitutive laws

We consider the *constitutive laws for the linear piezoelectricity* (see Eqs.(6)) applied for an orthotropic symmetry. On using the stress and electric induction resultants defined by Eqs.(13-16), we are able to put the constitutive equations for the generalized resultants in the matrix form

$$\begin{bmatrix} N_1 \\ N_2 \\ N_6 \end{bmatrix} = \begin{bmatrix} Q_{11} & Q_{12} & 0 \\ Q_{12} & Q_{22} & 0 \\ 0 & 0 & Q_{66} \end{bmatrix} \begin{bmatrix} S_1^{(0)} \\ S_2^{(0)} \\ S_6^{(0)} \end{bmatrix} + \begin{bmatrix} e_{31}^* \\ e_{32}^* \\ 0 \end{bmatrix} 2V \quad , \tag{22}$$

where we have set $Q_{ab} = hC_{ab}^*$ for $(ab) \in \{(11),(22),(12),(66)\}$ (the Voigt notation is used for convenience) and C_{ab}^* are the modified modulus of elasticity due to the zero normal shear stress hypothesis (σ_{33} negligeable), given by $C_{ab}^* = C_{ab}^E - C_{a3}^E C_{3b}^E / C_{33}^E$. We have the same for the piezoelectric and dielectric coefficients $e_{ja}^* = e_{ja} - e_{j3} C_{a3}^E / C_{33}^E$ and $\chi_{ij}^* = \chi_{ij} + e_{i3} e_{j3} / C_{33}^E$. We have also the following matrix form

$$\begin{bmatrix} M_1 \\ M_2 \\ M_6 \\ \hat{M}_1 \\ \hat{M}_2 \\ \hat{M}_6 \\ D_3^{(2)} \\ D_3^{(3)} \end{bmatrix} = \begin{bmatrix} D_{11} & D_{12} & 0 & d_{11} & d_{12} & 0 & R_{31} & r_{31} \\ & D_{22} & 0 & d_{12} & d_{22} & 0 & R_{32} & r_{32} \\ & & D_{66} & 0 & 0 & d_{66} & 0 & 0 \\ & & & \hat{D}_{11} & \hat{D}_{12} & 0 & \hat{R}_{31} & \hat{r}_{31} \\ & & & & \hat{D}_{22} & 0 & \hat{R}_{32} & \hat{r}_{32} \\ & & \text{(sym.)} & & & \hat{D}_{66} & 0 & 0 \\ & & & & & & P_{33} & \overline{P}_{33} \\ & & & & & & & \overline{\overline{P}}_{33} \end{bmatrix} \begin{bmatrix} S_1^{(1)} \\ S_2^{(1)} \\ S_6^{(1)} \\ S_1^{(2)} \\ S_2^{(2)} \\ S_6^{(2)} \\ \phi_2 \\ \phi_3 \end{bmatrix} \quad , \tag{23}$$

$$\begin{bmatrix} \hat{Q}_1 \\ \hat{Q}_2 \\ D_1^{(2)} \\ D_2^{(2)} \\ D_1^{(3)} \\ D_2^{(3)} \end{bmatrix} = \begin{bmatrix} \hat{A}_{55} & 0 & L_{15} & 0 & \overline{L}_{15} & 0 \\ & \hat{A}_{44} & 0 & L_{24} & 0 & \overline{L}_{24} \\ & & B_{11} & 0 & \overline{B}_{11} & 0 \\ & \text{(sym.)} & & B_{22} & 0 & \overline{B}_{22} \\ & & & & \overline{\overline{B}}_{11} & 0 \\ & & & & & \overline{\overline{B}}_{22} \end{bmatrix} \begin{bmatrix} \gamma_1 \\ \gamma_2 \\ \phi_{2,1} \\ \phi_{2,2} \\ \phi_{3,1} \\ \phi_{3,2} \end{bmatrix} \quad , \tag{24}$$

All the coefficients in Eqs.(23-24) are defined by

$$\begin{aligned}
&\left(D_{ab}, d_{ab}, \hat{D}_{ab}\right) = \left(\tfrac{1}{12}, \tfrac{2}{\pi^3}, \tfrac{1}{2\pi^2}\right) h^3 C^*_{ab} \quad , \\
&\left(R_{3\alpha}, r_{3\alpha}, \hat{R}_{3\alpha}, \hat{r}_{3\alpha}\right) = \left(\tfrac{h}{6}, -\tfrac{2}{\pi^2}, \tfrac{4h}{\pi^3}, -\tfrac{1}{2\pi}\right) h^2 e^*_{3\alpha} \quad , \\
&\left(P_{33}, \overline{P}_{33}, \overline{\overline{P}}_{33}\right) = \left(-\tfrac{h^2}{3}, \tfrac{4h}{\pi^2}, -\tfrac{1}{2}\right) h \chi^*_{33} \quad , \\
&\hat{A}_{MN} = \tfrac{h}{2} C^*_{MN} \quad , \\
&\left(L_{\alpha N}, \overline{L}_{\alpha N}\right) = \left(-\tfrac{4h}{\pi^2}, \tfrac{1}{2}\right) \tfrac{h^2}{\pi} e^*_{\alpha N} \quad , \\
&\left(B_{\alpha\alpha}, \overline{B}_{\alpha\alpha}, \overline{\overline{B}}_{\alpha\alpha}\right) = \left(-\tfrac{h^2}{30}, \tfrac{4h}{\pi^4}, -\tfrac{1}{2\pi^2}\right) h^3 \chi^*_{\alpha\alpha} \quad ,
\end{aligned}$$

with $\alpha \in \{1,2\}$, $(MN) \in \{(44),(55)\}$ and $(\alpha N) \in \{(24),(15)\}$. In addition, the strain tensors which have been introduced in Eqs.(23-24) are defined by $S^{(0)}_{\alpha\beta} = U_{(\alpha,\beta)}$, $S^{(1)}_{\alpha\beta} = -w_{,\alpha\beta}$ and $S^{(2)}_{\alpha\beta} = \gamma_{(\alpha,\beta)}$ and we use the appropriate Voigt notation, next. It should be observed from the constitutive laws for the generalized resultants that if an electric potential is applied on the top and bottom faces of the plate, an elongation or compression will be produced only (see Eq.(22)).

7. Solution for piezoelectric plates in cylindrical bending

Now, we possess all the necessary ingredients to solve the plate problem. On substituting the constitutive laws (22)-(24) into the plate equations (19)-(20), we are able to write down the equations in terms of the unknown fields $\{U_1, U_2, w, \gamma_1, \gamma_2, \phi_2, \phi_3\}$. Next, we consider a *surface density of normal load* on the top face and *electric potential* imposed on the top and bottom surfaces of the plate. The shear traction is zero on the top and bottom faces ($f_\alpha = 0$). In addition, there is no surface moment density ($\hat{m}_\alpha = 0$). The *simple support conditions* for a rectangular plate of length L are simulated by $\sigma_{11}(0,z) = \sigma_{11}(L,z) = 0$, $\sigma_{13}(0,z) = \sigma_{13}(L,z) = 0$ and $u_3(0,z) = u_3(L,z) = 0$ (Fig.1). All stresses, strains, displacements, electric field and potential do not depend on the y variable and the displacement u_2 plays any role in the problem, it can be dropped out ($u_2 = 0$, $\gamma_2 = 0$). The electromechanical load functions can be expressed in the form of Fourier series as follows

$$(p(x), V(x)) = \sum_{n=1}^{\infty} (S_n, V_n) \sin \lambda_n x \quad , \tag{25}$$

with

$$\lambda_n = n\pi/L, \qquad S_n = 4S_0/n\pi, \qquad V_n = 4V_0/n\pi \quad . \tag{26}$$

The loads defined by Eq.(25) represent uniform applied surface density of force S_0 and electric potential V_0. A solution to Eqs.(19-20) along with the constitutive equations (22)-(24) which satisfies the boundary conditions of the cylindrical bending of a plate simply supported takes on the form

$$\begin{aligned}
(U_1(x), \gamma_1(x)) &= \sum_{n=1}^{\infty} (U_n, \Gamma_n) \cos \lambda_n x \quad , \\
(w(x), \phi_2(x), \phi_3(x)) &= \sum_{n=1}^{\infty} (W_n, \Phi_{2,n}, \Phi_{3,n}) \sin \lambda_n x \quad .
\end{aligned} \tag{27}$$

The Fourier coefficients in the above series are determined by putting the solution (27) into the plate equations and solving simultaneously a set of linear algebraic equations for each n. The set of linear algebraic equations takes on the matrix form

$$\begin{bmatrix} -\lambda_n^2 Q_{11} & 0 & 0 & 0 & 0 \\ & -\lambda_n^4 D_{11} & \lambda_n^3 d_{11} & -\lambda_n^2 R_{31} & -\lambda_n^2 r_{31} \\ & & -\left(\hat{A}_{55}+\lambda_n^2 \hat{D}_{11}\right) & \lambda_n\left(\hat{R}_{31}-L_{15}\right) & \lambda_n\left(\hat{r}_{31}-\overline{L}_{15}\right) \\ & \text{(sym.)} & & -\left(P_{33}+\lambda_n^2 B_{11}\right) & -\left(\overline{P}_{33}+\lambda_n^2 \overline{B}_{11}\right) \\ & & & & -\left(\overline{\overline{P}}_{33}+\lambda_n^2 \overline{\overline{B}}_{11}\right) \end{bmatrix} \begin{bmatrix} U_n \\ W_n \\ \Gamma_n \\ \Phi_{2,n} \\ \Phi_{3,n} \end{bmatrix} = \begin{bmatrix} -2\lambda_n e_{31}^* V_n \\ S_n \\ 0 \\ 0 \\ 0 \end{bmatrix}. \quad (28)$$

The matrix possesses real elements and is symmetric. Now the resolution of the problem consists of finding the Fourier coefficients by solving Eq.(28) and substituting the result into the Fourier series (27) to go back to the displacement field and electric potential. Afterwards, the stresses and the normal component of the electric displacement are also computed by using the constitutive equations (6) and taking the approximations defined by Eq.(7) into account.

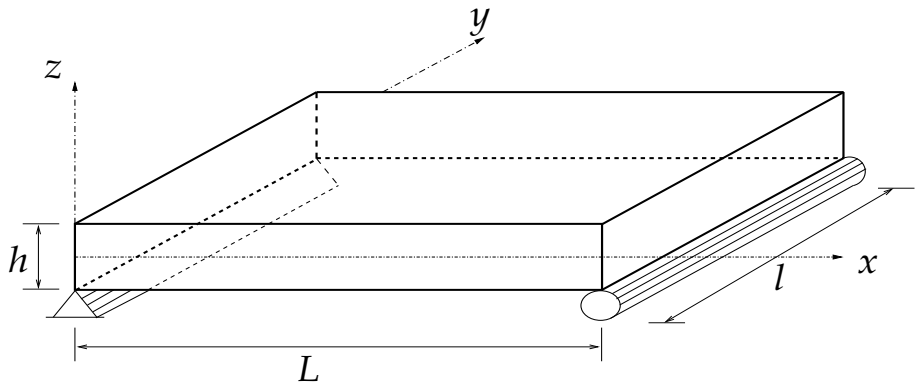

Fig.1 : *Piezoelectric plate on simple supports*

Numerical results for the single plate problem

We apply the above results to a single plate made of PZT-4 ceramics, whose the nonzero material constants are given in Table 1 [20]. The geometry of the plate is $L = 0.1\ m$ and the slenderness ratio is $L/h = 10$. The resulting displacements, stresses and electric potential are given in nondimensional unit as follows

(i) for the density of normal force $S_0 \neq 0$ ($S_0 = 1000\ N/m^2$), we set

$$(U, W, \Phi) = \frac{C_{11}}{hS_0}\left(u_1, u_3, \phi/E_0\right), \quad (T_{ij}, \mathcal{D}_l) = \frac{1}{S_0}\left(\sigma_{ij}, E_0 D_l\right) \quad ,$$

(ii) for a uniform electric potential $V_0 \neq 0$ ($V_0 = 50$ volts), we have

$$(U, W, \Phi) = \frac{E_0}{V_0}\left(u_1, u_3, \phi/E_0\right), \quad (T_{ij}, \mathcal{D}_l) = \frac{hE_0}{C_{11}V_0}\left(\sigma_{ij}, E_0 D_l\right) \quad .$$

For the present numerical illustration we take $E_0 = 10^{10}$ volts/m. Only 30 terms are retained in series (25) for the applied force density and 50 terms for the applied electric potential in order to ensure the convergence. The results obtained in the case of a plate subject to a uniform normal load S_0 are presented in Fig.2 in dimensionless variables. The plate, in this case, undergoes a bending. In Fig.2.a, the displacement U at $x = 0$ is almost

	C_{11}^E (GPa)	C_{12}^E	C_{33}^E	C_{13}^E	C_{44}^E	e_{31} (C/m^2)	e_{33}	e_{15}	χ_{11} (nF/m)	χ_{33}
PZT-4	139.	77.8	115.	74.3	25.6	-5.2	15.1	12.7	13.06	11.51
ZnO	209.7	210.9	121.1	105.1	42.5	-0.61	1.14	-0.59	0.074	0.078

Table 1: *Independent elastic, piezoelectric and dielectric constants of piezoelectric materials (transversely isotropic symmetry).*

linear through the plate thickness. The flexural displacement W at $x = L/2$ is given in Fig.2.b, the straight line corresponds to the plate model, but the discrepancy between the maximum value of the deflection for the 3D computation and that of the 2D model is less than 1 %. The most interesting curve is the electric potential at the plate center given in Fig.2.c, this is the induced electric potential through the piezoelectric coupling by the elastic deformation. This ascertains the existence of the ϕ_2 term in the electric potential expansion (7). The stress component T_{11} at $x = L/2$ is drawn in Fig.2.d. We observe a pretty good agreement with the results obtained with *finite element computations*. The latter have been performed with ABAQUS code using 8-node tetrahedral elements and 3600 elements have been considered.

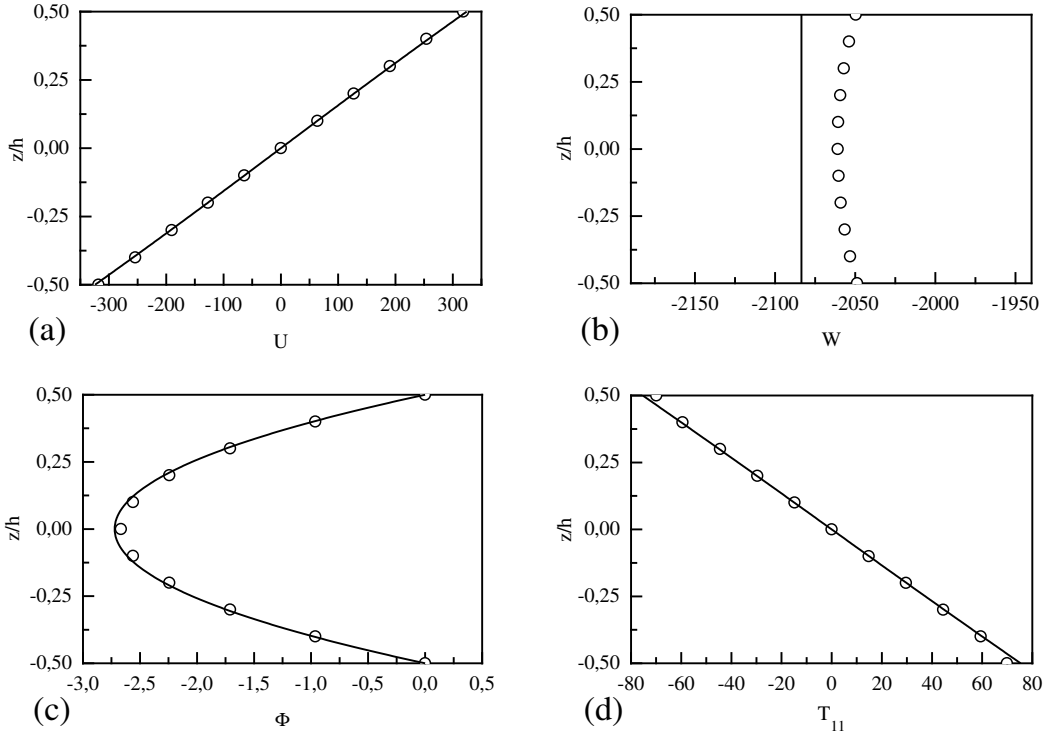

Fig.2 : *Force density applied on the top face of a piezoelectric single plate 2D model (full line) and finite element (small circles)*

Regarding the case of an applied electric potential, the results are collected together in Table 2 for the displacement U at $x = L$, the electric displacement $\mathcal{D}_3$ and the stress T_{22} at the plate center. Note that, in this simple situation, there is no deflection ($W = 0$), an elongational deformation along the x-axis is only produced. In this situation, a thickness deformation is obviously produced for the 3D plate problem due to the piezoelectric

	2D model	Finite element	difference
U	-16.2	-16.42	1.4 %
T_{22}	-1.477	-1.447	2 %
$\mathcal{D}_3$	-23.42	-22.96	2 %

Table 2: *Single piezoelectric plate, applied electric potential.*

constant e_{33}. The present plate approach does not account for the thickness variation since the deflection w is constant through the plate thickness. In spite of this limitation, the thickness variation represents however less than 1 % of the elongation or compression in the direction of the plate length. The deflection approximation could be improved by setting $u_3(x,y,z) = w(x,y) + h(z)\, w_1(x,y)$ where $h(z)$ is an appropriate function which must satisfy some boundary conditions on the top and bottom faces of the plate.

8. Bilayered piezoelectric structure

8.1. General formulation

Here, we are concerned with a plate made of *two piezoelectric layers* of different thicknesses and materials. The main difficulty, in the model, is the interface continuity of certain mechanical and electrical quantities. In this situation, the present approach combines an *equivalent single-layer* theory for the mechanical displacements with a *layerwise-type approximation* for the electric potential. Accordingly, the approximation for the elastic displacements defined by Eqs.(7) is still valid while the electric potential is assumed to be of the form

$$\phi^{(\ell)}(x,y,z) = \phi_0^{(\ell)}(x,y) + z_\ell \phi_1^{(\ell)}(x,y) + P_\ell(z_\ell)\phi_2^{(\ell)}(x,y) + g(z)\phi_3^{(\ell)}(x,y) \quad , \qquad (29)$$

with $\ell = 1$ or 2 corresponding to the lower or upper layer, respectively and where $P_\ell(z) = z^2 - (h_\ell/2)^2$ and $g(z)$ is still defined by Eq.(8). The potential is defined in the local coordinates of the layer where z_ℓ is the thickness coordinate with respect to the mid-plane of the ℓth layer while z is the thickness coordinate measured from the laminate geometric mid-plane (see Fig.3).

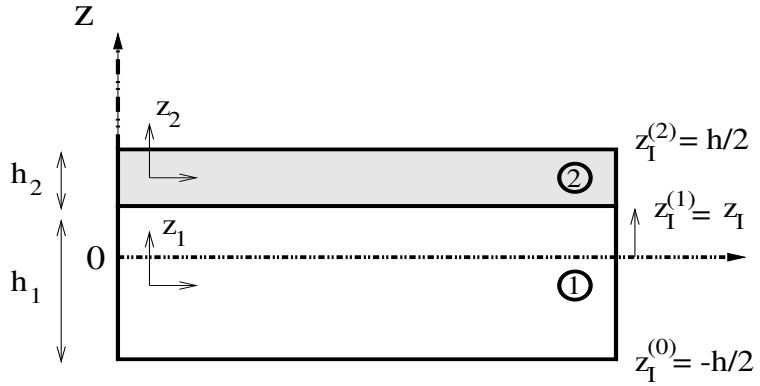

Fig.3 : *Piezoelectric bilayer plate*

The variable change is given by

$$z_1 = z + h_2/2 \qquad \text{and} \qquad z_2 = z - h_1/2 \quad .$$

Next, we discuss the continuity conditions. It is clear that the elastic displacements are continuous at $z = z_I = \frac{1}{2}(h_1 - h_2)$. However, the continuity of the electric potential as well as the normal component of the electric displacement must be imposed, which can be written as

$$\left\{ \begin{array}{l} \mathcal{A} = \phi^{(1)}(x, y, z_I) - \phi^{(2)}(x, y, z_I) = 0 \quad , \\ \mathcal{B} = D_3^{(1)}(x, y, z_I) - D_3^{(2)}(x, y, z_I) = 0 \quad . \end{array} \right. \tag{30}$$

Moreover, the boundary conditions for the electric potential on the top and bottom faces of the plate must be satisfied and they are given by

$$\left\{ \begin{array}{l} \phi^{(1)}(x, y, -h/2) = \phi_0^{(1)} - \frac{h_1}{2}\phi_1^{(1)} = -V \quad , \\ \phi^{(2)}(x, y, +h/2) = \phi_0^{(2)} + \frac{h_2}{2}\phi_1^{(2)} = +V \quad . \end{array} \right. \tag{31}$$

Now, the study amount to finding the set of unknown functions $\{U_1, w, \gamma_1, \phi_1^{(\ell)}, \phi_2^{(\ell)}, \phi_3^{(\ell)}; \ell \in \{1, 2\}\}$ subject to the continuity conditions (30). In order to account for the conditions (30) in the variational formulation we introduce *Lagrange multipliers* λ and μ in the Hamilton principle. Then the virtual works due to the *continuity conditions*

$$\delta \int_{t_1}^{t_2} \int_{\Sigma} (\lambda \mathcal{A} + \mu \mathcal{B})\, dS dt \quad , \tag{32}$$

must be added to the formulation (11). The variation of the Lagrange multipliers leads to the conditions (30), but additional terms containing the Lagrange multipliers appear in the plate equations. As consequence, the Lagrange multiplers are considered as unknown functions and a total of 11 unknown quantities should be determined for the bilayer problem.

8.2 - Numerical results for the piezoelectric bimorph.

An interesting and practical situation can be considered [21]. In this situation, both piezoelectric layer are made of the identical material and have the same thicknesses, however, the piezo-active axes are in opposite directions. When an electric potential is then applied to the bimorph, one layer elongates while the other one shrinks, resulting in a global bending of the plate. As in the single plate case, the bimorph structure is assumed to be simply supported. The hypotheses for the single plate hold in the present case. The same form for the electromechanical loads is considered (see Eq.(25)) and solutions to the bimorph equations are searched for in the Fourier series (see Eq.(27)).

The numerical results are collected in Fig.4 in dimensionless variables as defined in the single plate problem. In a first situation, the bimorph structure, composed of PZT-4 material, undergoes an applied force density on the top face with the electric potential and shear stresses at the top and bottom faces specified to be zero. The elongational displacement U at $x = 0$ is shown in Fig.4.a. The flexural displacement W at $x = L/2$ is presented in Fig.4.b, as in the single plate case, the straight line corresponds to the plate model, nevertheless the discrepancy between the maximum values of the deflection, at the center of the plate, for the plate approximation and the finite element computation for the 3D model is less than 1 %. Figure 4.c provides the through-thickness distribution of the induced electric potential at $x = L/2$, the latter is very close to the 3D computation. Finally the stress T_{11} also at $x = L/2$ is plotted in Fig.4.d, exhibiting the usual discontinuity at the interface. A rather good accuracy is observed for the present plate approach in comparison to the results obtained from the finite element method.

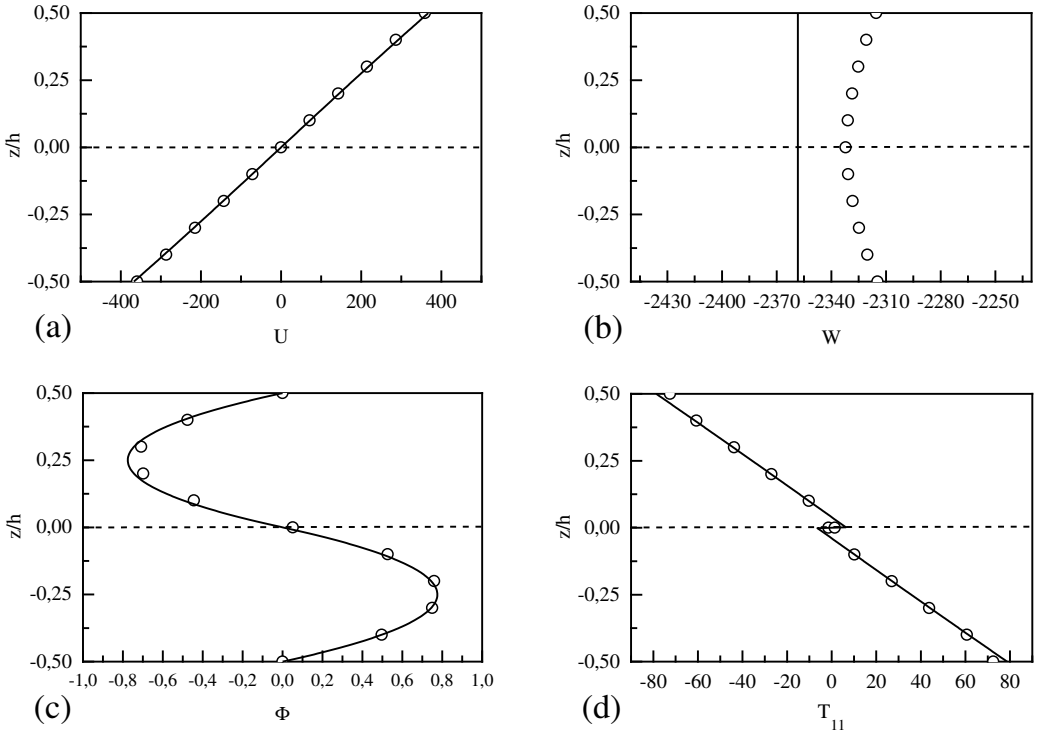

Fig.4 : *Force density applied on the top face of a piezoelectric bimorph 2D model (full line) and finite element (small circles)*

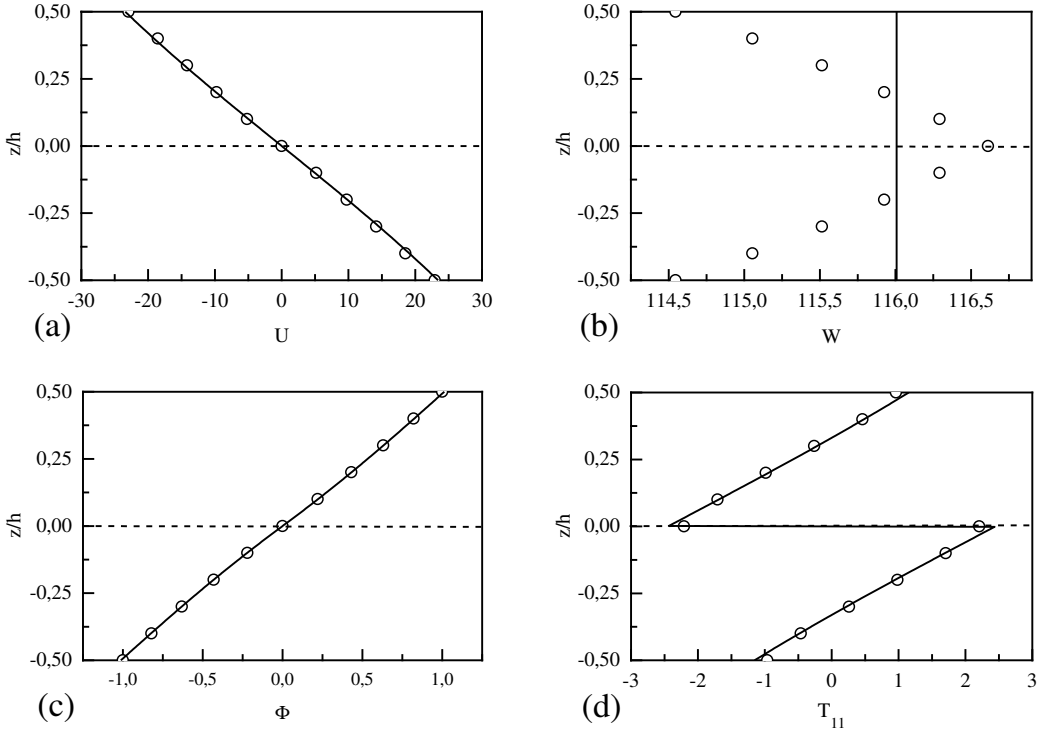

Fig.5 : *Applied electric potential to a piezoelectric bimorph 2D model (full line) and finite element (small circles)*

A second series of results are presented in Fig.5 for the case of an applied electric potential at the top and bottom faces of the bimorph structure. Here, in Fig.5.a we have the through-thickness distribution of the longitudinal displacement U at $x = 0$ which is almost linear including small shear effects. The induced flexural displacement W at the plate center is displayed in Fig.5.b. The electric potential at $x = L/2$ is given in Fig.5.c and the stress component T_{11} also at $x = L/2$ is plotted in Fig.5.d. In this situation, we note a good agreement of the through-thickness distribution with the corresponding results provided by the finite element computations. In dimensional units, the deflection displacement produced by an applied electric potential of 100 volts is of the order 0.6 μm at the plate center. Larger deflections can be obtained with higher voltages and larger slenderness ratios.

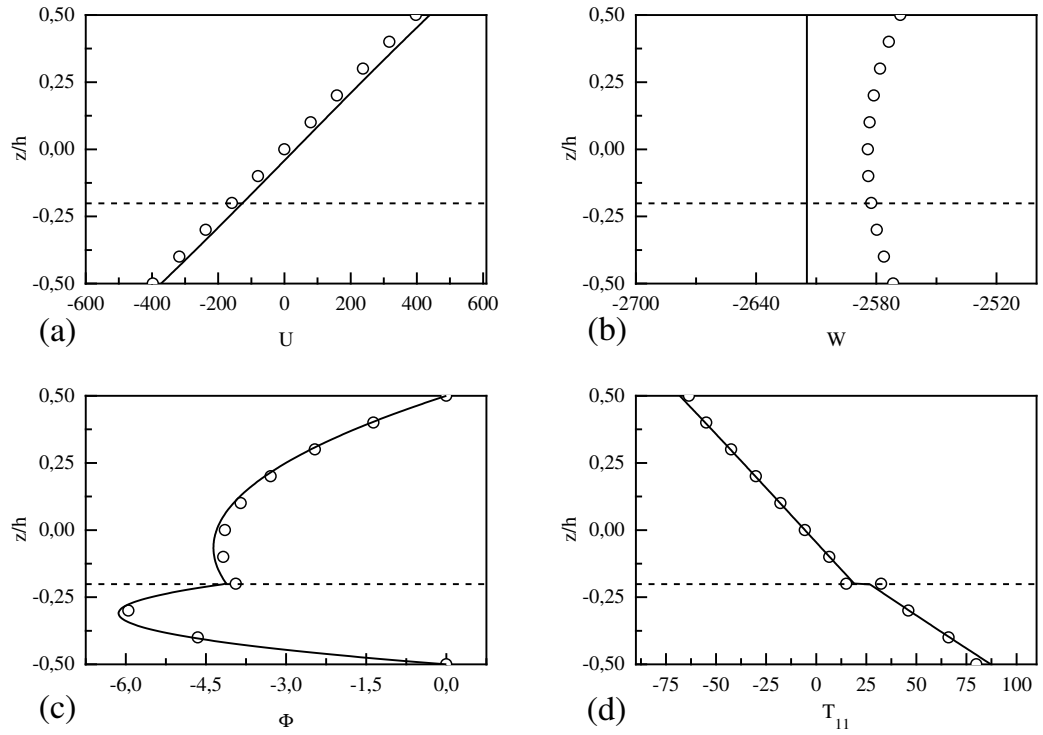

Fig.6 : *Force density applied on the top face of a piezoelectric bilayer plate 2D model (full line) and finite element (small circles)*

8.3 - Numerical results for the piezoelectric bilayer.
Here, we briefly summerize the results for a plate made of two piezoelectric layers of different materials and thicknesses. The lower layer is made of ZnO piezoelectric crystal with $h_1 = 0.3h$ while the upper layer consists of PZT-4 piezoelectric material with $h_2 = 0.7h$. Two situations are considered. (i) Applied force density at the top surface of the plate : the distributions of the elongational displacement at $x = 0$, deflection displacement, electric potential and stress component T_{11} at $x = L/2$ along the plate thickness are presented in Fig.6.a, b, c and d, respectively. (ii) Applied electric field at the top and bottom faces of the plate : the induced elongational displacement at $x = 0$, electric potential, stress component T_{11} and electric displacement component $\mathcal{D}_3$ at $x = L/2$ are drawn in Fig.7.a, b, c and d, respectively. It is worthwhile noting the rather good accuracy of the results in comparison to those provided by the finite element computation performed on the 3D piezoelectric body. An additional comparison can be done to an exact solution for

laminated piezoelectric plates in cylindrical bending which is merely an extension of the Pagano's works for elastic laminates [22] to piezoelectric plates [23].

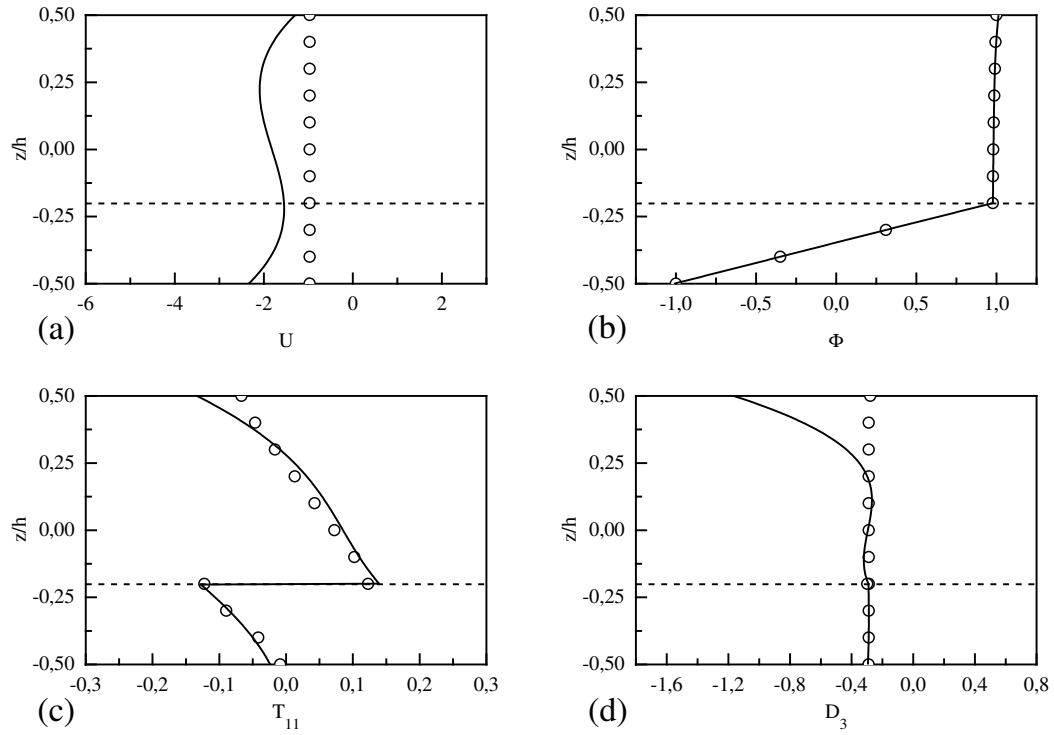

Fig.7 : *Applied electric potential to a piezoelectric bilayer plate 2D model (full line) and finite element (small circles)*

9. Closing remarks.

In this paper, an approximation theory for laminated plates including piezoelectric layers is presented. The model is based on the combination of an *equivalent single-layer approach* for the mechanical displacement with a *layerwise-type modelling* for the electric potential. Moreover, the theory accounts for the shearing effects, which play an important role in the accuracy of the results. The approach thus presented, here, has been tested for two kinds of electromechanical loads (force density and electric potential) applied on faces of the laminate. A complete set of coupled equations for the generalized stress resultants (membrane resultant and moments) and electric inductions is obtained from a variational formulation accounting for the continuity conditions at the layer interfaces by means of Lagrange multipliers. The latter procedure is more elegant than the use of the equations of continuity to reduce the number of unknowns. In order to ascertain the validity of our piezoelectric plate approach, we have considered some numerics for (i) a single piezoelectric plate, (ii) a piezoelectric bimorph and (iii) a plate composed of two different piezoelectric layers for an applied normal force density at the top surface of the plate and applied electric potential at the top and bottom faces of the laminate. The results indicate that the present model provides some interesting comparisons to the results obtained from the finite element computations for the full 3D model. The through-thickness distributions for the mechanical and electric quantities are computed with quite good accuracy (discrepancy less than 2 %). One of the limitations is that the averaged transverse shear stress over the plate thickness can be only estimated in the framework of the present

approach. Nevertheless, the model can be improved by introducing a layerwise approach for the mechanical quantities in order to ascertain the shear stress continuity at the layer interfaces.
Finally, in view of these first results, we are encouraged to extend the present approach to the study of vibrations of piezoelectric laminated plates [24]. Some other boundary conditions can be considered, for instance, applied electric charges on the plate faces or applied electric potential at the layer interfaces. The case of clamped plates is also an interesting and practical situation to be examined. Some of these extensions will be investigated in further works.

Acknowledgements - The authors are very grateful to the "Centre de Mécanique des Milieux Continus" at the University of "Versailles/Saint-Quentin-en-Yvelines" which has allowed them to make use of ABAQUS code for the finite element computations.

References

1. Rao S.S., Sunar M. Piezoelectricity and its use in disturbance sensing and control of flexible structures : A survey. *ASME Appl. Mech. Rev.* 1994; **47**: 113-123.
2. Peters D.J., Blackford B.L. Piezoelectric bimorph-based translation device for two-dimensional, remote micropositioning. *Rev. Sci. Instrum.* 1989; **60**: 138-140.
3. Loewy R.G. Recent developments in smart structures with aeronautical applications. *Smart Mater. Struct.* 1997; **6**: R11-R42.
4. Hagoud N.W., Chung W.H., Von Flotow A. Modelling of piezoelectric actuator dynamics for active structural control. *J. of Intell. Mater. Syst. and Struct.* 1990; **1**: 327-354.
5. Tiersten H.F. *Linear piezoelectric plate vibrations* (Plenum, New York, 1969).
6. Mindlin R.D. High frequency vibrations of piezoelectric crystal plates. *Int. J. Solids Structures* 1972; **8**: 895-906.
7. Lee C.K. Theory of laminated piezoelectric plates for the design of distributed sensors / actuators. Part 1 : Governing equations and reciprocal relationships. *J. Acoust. Soc. Am.* 1990; **87**: 1144-1158.
8. Zhang X.D., Sun C.T. Formulation of an adaptive sandwich beam. *Smart Mater. Struct.* 1996; **5**: 814-823.
9. Mitchell J.A., Reddy J.N. A refined hybrid plate theory for composite laminates with piezoelectric laminae. *Int. J. Solids Structures* 1995; **32**: 2345-2367.
10. Touratier M. An efficient standard plate theory. *Int. J. Engng. Sci.* 1991 **29**: 901-916.
11. Love A.E.H. *Treatise on the mathematical theory of elasticity.* New York, Dover, 1944.
12. Reissner E. On transverse bending of plates including the effect of transverse shear deformation. *Int. J. Solids Structures* 1975; **11**: 569-573.
13. Levinson M. An accurate, simple theory of static and dynamics of elastic plates. *Mech. Res. Comm.* 1980; **7**: 342-350.
14. Reddy J.N. A simple higher-order theory for laminated composite plates. *ASME J. Appl. Mech.* 1984; **51**: 745-752.
15. Touratier M. A refined theory of laminated shallow shells. *Int. J. Solids Struct.* 1992; **29**: 1401-1415.
16. Yang J.S. Equations for the extension and flexure of electroelastic plates under strong electric fields. *Int. J. Solids Structures* 1999; **36**: 3171-3192.
17. Rogacheva N.N. *The theory of piezoelectric shells and plates.* Boca Raton, CRC Press 1994.

18. Robbins D.H., Reddy J.N. Modelling of thick composites using a layerwise laminate theory. *Int. J. Num. Methods Engng.* 1993; **36**: 655-677.
19. Eringen A.C., Maugin G.A. *Electrodynamics of continua .I. Foundations and solid media* (Springer-Verlag, New York, 1990).
20. Berlincourt D.A., Curran D.R., Jaffe H. Piezoelectric and piezomagnetic materials and their function in transducers. In W.P. Mason Editor. *Physical Acoustics*, **vol.1**, 1964, p.169-270.
21. Smits J.G., Dalk S.I. and Cooney T.K. The constituent equations of piezoelectric bimorphs. *Sensors and Actuators* 1991; **A28**: 41-61.
22. Pagano N.J. Exact solutions for composite laminates in cylindrical bending. *J. Composite Materials* 1969; **3**: 398-411.
23. Heyliger P., Brooks S. Exact solutions for laminated piezoelectric plates in cylindrical bending. *J. Applied Mech.* 1996; **63**: 903-910.
24. Heyliger P., Brooks S. Free vibration of piezoelectric laminates in cylindrical bending. *Int. J. Solids Structures* 1995; **32**: 2945-2960.